Application of the Phase Compensation Method for the Design of a DC/AC Converter Based Stabilizer to Damp Inter-Area Power Oscillations

Application of the Phase Compensation Method for the Design of a DC/AC Converter Based Stabilizer to Damp Inter-Area Power Oscillations

W. Du, H. F. Wang *Senior Member*, J. Cao, H. F. Li and L Xiao

***Abstract* — The phase compensation method was proposed based on the concept of the damping torque analysis (DTA). It is a method for the design of a PSS (power system stabilizer) to suppress local-mode power oscillations in a single-machine infinite-bus power system. This paper presents the application of the phase compensation method for the design of a DC/AC converter based stabilizer to damp inter-area mode power oscillations in a multi-machine power system. The application is achieved by examining the direct damping contribution of the stabilizer to inter-area power oscillations without relying on DTA. The simplicity and localization of the phase compensation method are retained in the application presented in the paper, as the design requires only locally available transmission line information and DC/AC converter unit parameters.**

***Index Terms* — DC/AC converter, phase compensation method, power system small-signal stability, stabilizer**

I. Introduction

Damping torque analysis (DTA) was introduced by deMello and Concordia [1] on the basis of the Phillips-Heffron model [2] for a single-machine infinite-bus power system. It was further developed by Larsen and Swann [3] into the well-known phase compensation method for the design of a power system stabilizer (PSS). Since the 1980s, there has been a lot of effort to extend the phase compensation method to design PSSs [4-6] and FACTS stabilizers [7,8] in a multi-machine power system. However, because DTA is closely associated with the generators rotor motion, the extension of the phase compensation method requires the inclusion of complex dynamics from each of the generators in the multi-machine power system. The simplicity of the method proposed for a single-machine infinite-bus power system is therefore lost when extended to a multi-machine context, as the damping torque contribution to all generators needs to be considered [4-8]. Normally design of a stabilizer cannot be achieved locally as the global model of the entire multi-machine power system needs to be established.

A more recent work by Gurrala and Sen [9] proposed using the secondary bus voltage of generators step-up transformer to derive a Phillips-Heffron model to apply the phase compensation method for the PSS design. Though the design is still based on the concept of DTA, application to a multi-machine power system not only keeps the simplicity of the phase compensation method, but also does not require the complete power system information, which in practice may not always be readily available and is difficult to be validated when the system is large and complex. However, the proposed approach in [9] is to design the PSS to damp generator-versus-system (hence local-mode) power oscillations. It cannot thus be applied for the suppression of inter-area power oscillations.

This paper proposes application of the phase compensation method for the design of a DC/AC converter based stabilizer to suppress inter-area power oscillations in a multi-machine power system. The proposed application is established on the direct examination of damping contribution from the stabilizer to the inter-area power oscillations without relying on the concept of DTA. It does not involve explicit consideration of the complex dynamic interactions of generators. Furthermore, there is no need to obtain and validate the complete power system information to apply the phase compensation method because the design only requires the locally available parameters of the transmission lines and DC/AC converter based unit. Hence both the simplicity and localization of the phase compensation method to design the stabilizer is retained in the proposed application.

In the paper, two examples of multi-machine power systems installed with a static synchronous compensator (STATCOM) stabilizer and a battery energy storage system (BESS) stabilizer are presented. The stabilizers are designed to suppress inter-area power oscillations by using the method proposed in the paper. Results of modal analysis and non-linear simulation are given to confirm the effectiveness of the stabilizers. The purpose of the examples is to demonstrate the proposed application of the phase compensation method, rather than to confirm the effectiveness of the DC/AC converter based stabilizers or to compare them with other types of stabilizers, such as PSS and FACTS stabilizers. This is because the usefulness of the DC/AC converter based stabilizers to damp power system oscillations has been well presented in many previous publications, for example the STATCOM stabilizer [10,11] and the BESS stabilizer [12,13].

W. Du was with the Southeast University, Nanjing China, and is currently working at Queen's University of Belfast, Belfast, UK (e-mail: ddwenjuan@googlemail.com). Prof. H F Wang and Mr. J Cao are with Queen's University of Belfast, Belfast, UK. Dr. H. F. Li is with the Jiangsu Power Company, Nanjing, China. Prof. L Xiao is with the Institute of Electrical Engineering, Chinese Academy of Sciences, Beijing, China.

II. APPLICATION OF PHASE COMPENSATION METHOD IN A MULTI-MACHINE POWER SYSTEM

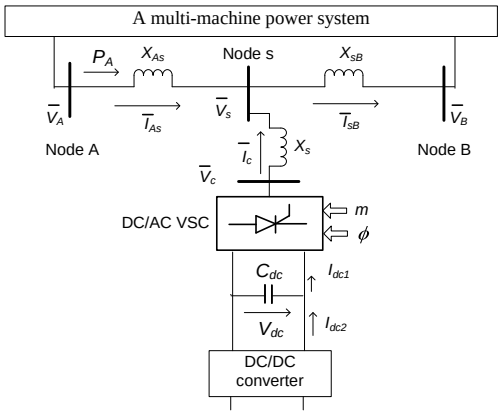

Figure 1 A DC/AC converter based unit in a multi-machine power system

Figure 1 shows that a DC/AC converter based unit is connected along a transmission line from node A to B in a multi-machine power system where $\bar{V}_A = V_A \angle \delta_A$ and $\bar{V}_B = V_B \angle \delta_B$. The DC/DC converter can be connected to an energy storage system, such as a BESS, or a renewable power generation plant, such as a PV power station. Without the DC/DC converter ($I_{dc2} = 0$), the unit is a STATCOM where there is no exchange of active power between the unit and the rest of the power system. The modulation ratio and phase of the DC/AC converter is m and ϕ respectively. A stabilizing signal can be superimposed on m to damp inter-area power oscillations along the transmission line between node A and B [10, 11, 14, 15]. When the unit is an energy storage system or a renewable power generation plant, it is of the capability to release and absorb active power. Thus the stabilizing signal can also be added on ϕ to suppress the line power oscillations via regulating the direct exchange of active power between the unit and the rest of the power system [12, 13].

In a single-machine infinite-bus power system, line power oscillations are closely related to the rotor motion of the synchronous generator which is connected at one end of the transmission line. Acceleration and deceleration of the generator absorbs and releases active power in dynamic response to the power oscillations. Hence DTA can be applied straightforwardly as the suppression of line power oscillations is equivalent to the damping of the rotor motion. However, in the DC/AC converter based unit in Figure 1, there is no rotating element closely related to the inter-area power oscillation frequencies. The problem of suppression of the line power oscillations cannot be directly converted into the damping of rotational motion within the unit. Instead, application of DTA to a DC/AC converter based stabilizer has to be carried out in two steps [5-8]. Firstly, by using the dynamic connections between the stabilizer and the generators, the damping torque contribution from the stabilizer to each of generators needs to be derived. Secondly the damping torque contribution to the generators is related to the damping of inter-area power oscillation modes. It is obvious that the complexity of applying DTA in the multi-machine power system has significantly increased. Moreover, a global mathematical model of the entire multi-machine power system must also be established for the application.

In fact, in the single-machine infinite-bus power system, the damping contribution from the PSS to the local-mode line power oscillations (ΔP) can be examined directly from the following relation between ΔP and the PSS control [1,3,16].

$$\Delta P = C_{delta}\Delta\delta + D_{delta}\Delta\omega + \Delta T(\Delta u_{pss}) \qquad (1)$$

where the prefix Δ denotes the small increment of a variable, P is the electric power supplied by the generator, ω the rotor speed and δ the angular position of the rotor of the generator respectively, C_{delta} and D_{delta} are two constant coefficients, $T(\Delta u_{pss})$ the electric torque contribution from and u_{pss} the stabilizing signal of the PSS respectively. In Eq.(1) $C_{delta}\Delta\delta + D_{delta}\Delta\omega$ is the contribution of the variable (such as $\Delta\delta$) outside the PSS to the line power oscillations. This component does not need to be considered in the PSS design [1,3,16]. The DTA establishes the fact that if $T(\Delta u_{pss}) = D_{pss}\Delta\omega$ $(D_{pss} > 0)$, it is a positive damping component in the line power oscillations, ΔP . The phase compensation method is to ensure that the PSS is designed such that it only contributes a positive damping torque $D_{pss}\Delta\omega$ $(D_{pss} > 0)$ so as to effectively suppress the line power oscillations.

The work presented below is the extension of Eq. (1) to the case of the multi-machine power system of Figure 1 by examining the direct damping contribution from the DC/AC converter based stabilizer to the inter-area power oscillations, ΔP_A, by extending. Firstly Eq. (1) for the inter-area power oscillations, ΔP_A , is derived by considering the direct contribution from the stabilizer to ΔP_A. The derivation is presented in the next subsection by establishing a local linearized model of the DC/AC converter based unit related to line power oscillations. Secondly in subsection B, the positive damping component in ΔP_A is established by using the well-known equal area criterion and linearized $P - \delta$ curve without referring to DTA. It is proposed that the stabilizer is designed simply by applying the phase compensation method to supply a positive damping component to ΔP_A so as to effectively suppress the inter-area power oscillations.

A. Local linearized model of the DC/AC converter based unit related to line power oscillations

The voltage at the AC terminal of the DC/AC converter in Figure 1 is [15,17]

$$\bar{V}_c = mk_c V_{dc} \angle \gamma = mk_c V_{dc} \angle \varphi + \phi \qquad (2)$$

where k_c is a constant dependent on the converter structure and V_{dc} the DC voltage at the DC terminal of the DC/AC converter. The modulation phase, ϕ is the phase difference between $\bar{V}_c = V_c \angle \gamma$ and $\bar{V}_s = V_s \angle \varphi$ at node s, i.e, $\phi = \gamma - \varphi$. Therefore from Figure 1

$$\bar{V}_s = jX_{sB}\bar{I}_{sB} + \bar{V}_B = jX_{sB}[\bar{I}_{As} - (\frac{\bar{V}_S - \bar{V}_C}{jX_s})] + \bar{V}_B$$
$$= jX_{sB}\bar{I}_{As} - \frac{X_{sB}}{X_s}\bar{V}_s + \frac{X_{sB}}{X_s}\bar{V}_c + \bar{V}_B \quad (3)$$

which gives

$$\bar{V}_s = \frac{jX_{sB}}{1+\frac{X_{sB}}{X_s}}\bar{I}_{As} + \frac{X_{sB}}{X_s(1+\frac{X_{sB}}{X_s})}\bar{V}_c + \frac{\bar{V}_B}{1+\frac{X_{sB}}{X_s}} \quad (4)$$

Hence it can be obtained that

$$\bar{V}_A = jX_{As}\bar{I}_{As} + \bar{V}_s = j(X_{As} + \frac{X_s X_{sB}}{X_s + X_{sB}})\bar{I}_{As}$$
$$+ \frac{X_{sB}}{X_s + X_{sB}}\bar{V}_c + \frac{X_s}{X_s + X_{sB}}\bar{V}_B = jX\bar{I}_{As} + \bar{V}_a \quad (5)$$

where

$$X = (X_{As} + \frac{X_s X_{sB}}{X_s + X_{sB}})$$
$$\bar{V}_a = \frac{X_{sB}}{X_s + X_{sB}}\bar{V}_c + \frac{X_s}{X_s + X_{sB}}\bar{V}_B = a\bar{V}_c + b\bar{V}_B$$

From Eq. (5) and the phasor diagram of Figure 2, the active power delivered along the transmission line from node A to s in Figure 1 can be obtained

$$P_A = \frac{V_a V_A}{X}\sin\delta' = \frac{V_A}{X}(bV_B\sin\delta_{AB} + akmV_{dc}\sin\gamma)$$
$$= \frac{V_A}{X}bV_B\sin\delta_{AB} + \frac{V_A}{X}akmV_{dc}\sin(\varphi + \phi) \quad (6)$$

Hence

$$\Delta P_A = \frac{\partial P_A}{\partial \delta_{AB}}\bigg|_0 \Delta\delta_{AB} + \frac{\partial P_A}{\partial V_A}\bigg|_0 \Delta V_A + \frac{\partial P_A}{\partial V_B}\bigg|_0 \Delta V_B$$
$$+ \frac{\partial P_A}{\partial \varphi}\bigg|_0 \Delta\varphi + \frac{\partial P_A}{\partial V_{dc}}\bigg|_0 \Delta V_{dc} + \frac{\partial P_A}{\partial m}\bigg|_0 \Delta m + \frac{\partial P_A}{\partial \phi}\bigg|_0 \Delta\phi \quad (7)$$

where subscript 0 denotes the value at a given steady-state operating condition of the power system.

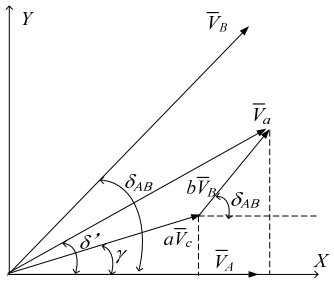

Figure 2 Phasor diagram in the common *X-Y* coordinate of the power system

In Appendix 1, the following equations are derived

$$\Delta V_s = a_{1f}\Delta V_{dc} + a_{2f}\Delta m + a_{3f}\Delta\phi$$
$$+ a_{4f}\Delta\delta_{AB} + a_{5f}\Delta V_A + a_{6f}\Delta V_B \quad (8)$$

$$\Delta\varphi = b_{1f}\Delta V_{dc} + b_{2f}\Delta m + b_{3f}\Delta\phi$$
$$+ b_{4f}\Delta\delta_{AB} + b_{5f}\Delta V_A + b_{6f}\Delta V_B \quad (9)$$

where a_{if} and $b_{if}, i = 1,2,3,4,5,6$ are constant coefficients. Substituting Eq. (9) into Eq. (7) gives

$$\Delta P_A = h_{AB}\Delta\delta_{AB} + h_A\Delta V_A + h_B\Delta V_B$$
$$+ h_{dc}\Delta V_{dc} + h_m\Delta m + h_f\Delta\phi \quad (10)$$

where h_{AB}, h_A, h_B, h_{dc}, h_m and h_f are constant coefficients. Eq. (10) indicates that the small-signal line power oscillation is directly affected by the variation of the line terminal variables, $\Delta\delta_{AB}$, ΔV_A and ΔV_B as well as the internal variables of the DC/AC converter unit, ΔV_{dc}, Δm and $\Delta\phi$.

From Figure 1, $\bar{V}_c = jX_s\bar{I}_s + \bar{V}_s$. Hence

$$I_{sd} = \frac{mkV_{dc}\sin\phi}{X_s}, I_{sq} = \frac{V_s - mkV_{dc}\cos\phi}{X_s} \quad (11)$$

where subscript d and q denotes the d and q component of the corresponding variables respectively in the d-q coordinate of the DC/AC converter based unit as shown by Figure 3. Linearization of the above equation is

$$\Delta I_{sd} = b_{1d}\Delta V_{dc} + b_{2d}\Delta m + b_{3d}\Delta\phi$$
$$\Delta I_{sq} = b_{1q}\Delta V_{dc} + b_{2q}\Delta m + b_{3q}\Delta\phi + b_{4q}\Delta V_s \quad (12)$$

The active power exchange between the converter based unit and the rest of the power system is

$$V_{dc}I_{dc1} = I_{sd}V_{cd} + I_{sq}V_{cq} \quad (13)$$

By using Eq. (2) and Figure 3, from Eq. (13) it can be obtained

$$V_{dc}I_{dc1} = I_{sd}mkV_{dc}\cos\phi + I_{sq}mkV_{dc}\sin\phi \quad (14)$$

Thus

$$I_{dc1} = I_{sd}mk\cos\phi + I_{sq}mk\sin\phi \quad (15)$$

Hence linearization of Eq. (15) can be obtained from Eq. (12)

$$\Delta I_{dc1} = b_{d1}\Delta V_{dc} + b_{d2}\Delta m + b_{d3}\Delta\phi + b_{d4}\Delta V_s \quad (16)$$

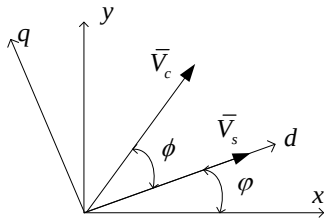

Figure 3 Phasor diagram in the d-q coordinate of the converter based unit

If the DC/AC converter-based unit in Figure 1 is an energy storage system or renewable generation plant, $I_{dc2} \neq 0$. The following state-space representation can be established

$$s\boldsymbol{X_P} = \boldsymbol{A_P}\boldsymbol{X_P} + \begin{bmatrix}\boldsymbol{b_P} & \boldsymbol{b_{vsc}}\end{bmatrix}\begin{bmatrix}\Delta V_{dc} \\ \Delta u_{vsc}\end{bmatrix} \quad (17)$$

$$\Delta I_{dc2} = \boldsymbol{C_P}\boldsymbol{X_P} + d_P\Delta V_{dc}$$

where $\boldsymbol{X_P}$ and u_{vsc} is the state variable vector and input of the energy storage or renewable generation unit respectively, $(\boldsymbol{A_P}, \begin{bmatrix}\boldsymbol{b_P} & \boldsymbol{b_{vsc}}\end{bmatrix}, \boldsymbol{C_P}, d_P)$ are the set of parameters of the state-space model of the unit.

The dynamic equation of the DC/AC converter is

$$\dot{V}_{dc} = \frac{1}{C_{dc}}(-I_{dc1} + I_{dc2}) \quad (18)$$

Hence by using Eq. (16) and (17), linearization of Eq.(18) can be obtained

$$s\Delta V_{dc} = b_1\Delta V_{dc} + b_2\Delta m + b_3\Delta\phi + b_4\Delta V_s + \boldsymbol{b_{dc}}\boldsymbol{X_P} \quad (19)$$

where $b_i, i = 1,2,3,4$ are constant coefficients and $\boldsymbol{b_{dc}}$ is a constant coefficient vector.

The DC/AC converter is controlled to regulate active and reactive power exchange between the converter-based unit and the rest of the power system. The two most popular control algorithms are the pulse width modulation (PWM) and the pulse amplitude modulation (PAM) [14,15,17]. There are different types of control arrangements for the DC/AC converter, such as current, power and voltage control. Without loss of generality, Figure 4 shows the configuration of a voltage control type of converter with the PWM algorithm [14,15,17]. A stabilizing signal $\Delta u_{pss}(m)$ can be added on the control loop of the modulation ratio signal m to improve the damping of power system oscillations. When the DC/AC converter based unit in Figure 1 is an energy storage system or renewable generation plant, a stabilizing signal $\Delta u_{pss}(\phi)$ can also be superimposed on the control loop of the modulation phase signal ϕ. In Figure 4, K_{pac}, K_{ac}, K_{pdc} and K_{dc} is the gain of the AC and DC voltage proportional and integral (PI) controller respectively.

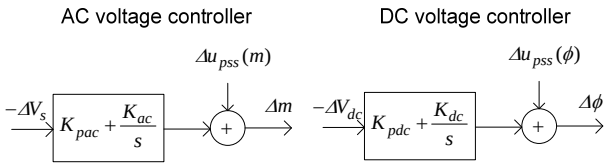

Figure 4 Configuration of voltage type PWM converter control

From Eq. (8), (10) and (19) and Figure 4, a local linearized model of the DC/AC converter-based unit related to line power oscillations can be constructed as shown by Figure 5. This model includes the dynamics of the DC/AC converter based unit. It describes line power oscillations as affected by various variables (input signals to the model) of the transmission line $\Delta\delta_{AB}$, ΔV_A and ΔV_B as well as Δu_{vsc} in the converter based unit, the stabilizing signals $\Delta u_{pss}(m)$ and $\Delta u_{pss}(\phi)$. According to the principle of superimposition of linear systems, from Figure 5,

$$\Delta P_A = \Delta P_A(\boldsymbol{\Delta E}) + \Delta P_A(\boldsymbol{\Delta u_{pss}}) \quad (20)$$

where

$$\begin{aligned}
&\Delta P_A(\boldsymbol{\Delta E}) = \begin{bmatrix} F_{AB}(s) & F_A(s) & F_B(s) & F_{vsc}(s) \end{bmatrix} \boldsymbol{\Delta E} \\
&\Delta P_A(\boldsymbol{\Delta u_{pss}}) = \begin{bmatrix} F_{pssm}(s) & F_{pssf}(s) \end{bmatrix} \boldsymbol{\Delta u_{pss}} \\
&\boldsymbol{\Delta E} = \begin{bmatrix} \Delta\delta_{AB} & \Delta V_A & \Delta V_B & \Delta u_{vsc} \end{bmatrix}^T, \\
&\boldsymbol{\Delta u_{pss}} = \begin{bmatrix} \Delta u_{pss}(m) & \Delta u_{pss}(\phi) \end{bmatrix}^T
\end{aligned} \quad (21)$$

where $F_{AB}(s)$, $F_A(s)$, $F_B(s)$, $F_{vsc}(s)$, $F_{pssm}(s)$ and $F_{pssf}(s)$ constitute the transfer function of the forward path from $\Delta\delta_{AB}$, ΔV_A, ΔV_B, Δu_{vsc}, $\Delta u_{pss}(m)$ and $\Delta u_{pss}(\phi)$ to ΔP_A respectively.

In the $\delta_{AB} - \Delta\dot{\delta}_{AB}$ coordinate, $\Delta P_A(\boldsymbol{\Delta E})$ can be decomposed,

$$\Delta P_A(\boldsymbol{\Delta E}) = C_{other}\Delta\delta_{AB} + D_{other}\Delta\dot{\delta}_{AB} \quad (22)$$

where C_{other} and D_{other} are two constant coefficients. Substituting Eq. (22) into Eq. (20) gives

$$\Delta P_A = C_{other}\Delta\delta_{AB} + D_{other}\Delta\dot{\delta}_{AB} + \Delta P_A(\boldsymbol{\Delta u_{pss}}) \quad (23)$$

Eq. (23) is the extended form of Eq. (1) in the multi-machine power system about line power oscillations. In Eq. (23), $C_{other}\Delta\delta_{AB} + D_{other}\Delta\dot{\delta}_{AB}$ represents the effect of system variables external to the stabilizers on line power oscillations, a term similar to $C_{delta}\Delta\delta + D_{delta}\Delta\omega$ in Eq. (1), and $\Delta P_A(\boldsymbol{\Delta u_{pss}})$ is the direct contribution from the stabilizers.

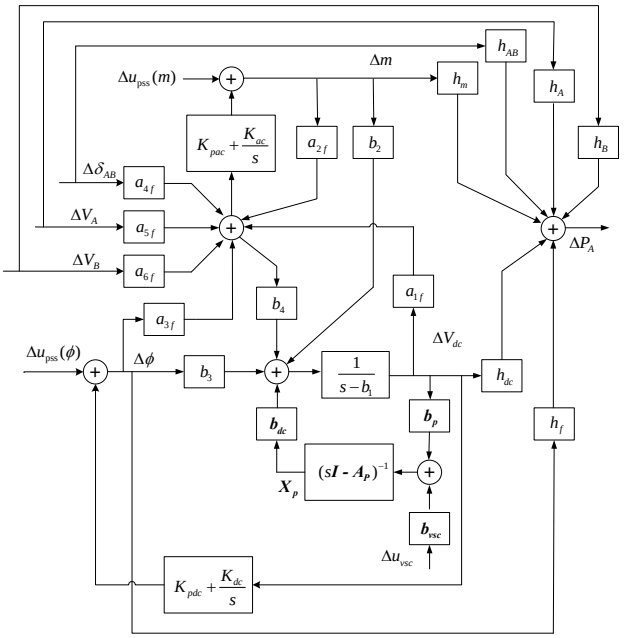

Figure 5 Local linearized model of a DC/AC converter based unit related to line power oscillations

B. Application of the phase compensation method

Figure 6 shows the linearized $P_A - \delta_{AB}$ curve where δ_{AB0}, P_{A0} determine the steady-state operating point of the power system. It is assumed that the small-signal oscillation of ΔP_A starts from point 'a' in Figure 6 with the operating point moving down. Without affecting the result of discussion, it is assumed that $D_{other} > 0$ in Eq.(23). When there is no stabilizing control, $\Delta P_A(\boldsymbol{\Delta u_{pss}}) = 0$ and Eq. (23) becomes

$$\Delta P_A = \Delta P_A(\boldsymbol{\Delta E}) = C_{other}\Delta\delta_{AB} + D_{other}\Delta\dot{\delta}_{AB} \quad (24)$$

which is shown by the dashed curve in Figure 6. This is because when the operating point moves down, $\Delta\dot{\delta}_{AB} < 0$. Hence $D_{other}\Delta\dot{\delta}_{AB} < 0$ is added on the line, $\Delta P_A(\boldsymbol{\Delta E}) = C_{other}\Delta\delta_{AB}$. When the operating point arrives at point 'f' and stops moving, $D_{other}\Delta\dot{\delta}_{AB} = 0$. Hence it should

be on the line, $\Delta P_A = \Delta P_A(\Delta \boldsymbol{E}) = C_{other}\Delta\delta_{AB}$. According to the equal area criterion, area '*ade*' is equal to that of '*dgf*'.

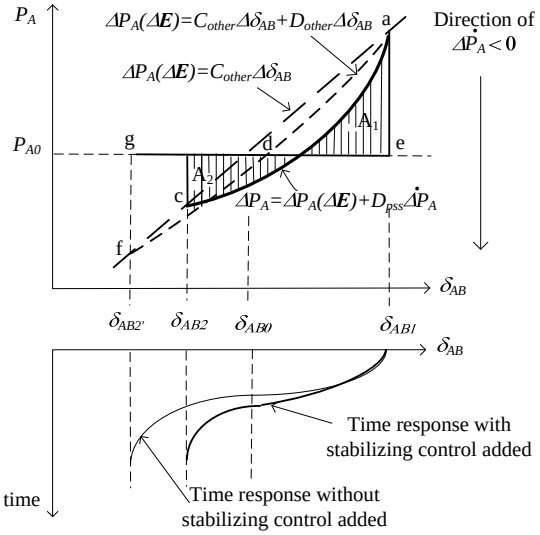

Figure 6 $P_A - \delta_{AB}$ curves and time response of δ_{AB}

When the stabilizing control is added and is set as

$$\Delta P_A(\Delta \boldsymbol{u}_{\boldsymbol{pss}}) = D_{pss}\Delta\dot{P}_A (D_{pss} > 0) \qquad (25)$$

where $\Delta\dot{P}_A$ denotes the time derivative of ΔP_A. According to Eq. (23), $D_{pss}\Delta\dot{P}_A < 0$ (for $\Delta\dot{P}_A < 0$) is added on the dashed curve $\Delta P_A(\Delta \boldsymbol{E}) = C_{other}\Delta\delta_{AB} + D_{other}\Delta\dot{\delta}_{AB}$ when the operating point moves down. Hence the operating point should move below the dashed curve along the highlighted trajectory in Figure 6. When the operating point stops on the line, $\Delta P_A(\Delta \boldsymbol{E}) = C_{other}\Delta\delta_{AB}$, area A_1 is equal to area A_2 at point 'c' where $\Delta\dot{P}_A = 0$ and $D_{other}\Delta\dot{\delta}_{AB} = 0$. It is apparent that $\delta_{AB1} - \delta_{AB0} > \delta_{AB0} - \delta_{AB2}$ which indicates extra positive damping provision from the stabilizing control to the power oscillation. A similar analysis can be carried out to examine the case when the operating point moves up from point 'c'.

Therefore, if ΔP_A is used as the feedback signal of the converter based stabilizer and the transfer function of the stabilizer is constructed by a lead-lag network, which is normally used by a PSS,

$$\Delta u_{pss}(x) = K_{pss}\frac{sT_w}{1+sT_w}\frac{1+sT_2}{1+sT_1}\frac{1+sT_4}{1+sT_3}\Delta P_A \qquad (26)$$

where $\Delta u_{pss}(x)$ is $\Delta u_{pss}(m)$ or $\Delta u_{pss}(\phi)$. From Eq. (21)

$$\Delta P_A(\Delta \boldsymbol{u}_{\boldsymbol{pss}}) = \begin{bmatrix} F_{pssm}(s) & F_{pssf}(s) \end{bmatrix}\begin{bmatrix} \Delta u_{pss}(m) \\ \Delta u_{pss}(\phi) \end{bmatrix} \qquad (27)$$

Thus according to Eq. (25), (26) and (27) parameters of the stabilizer can be set at the angular inter-area power oscillation frequency ω_{area} to satisfy the following equation

$$F_{pssx}(s)K_{pss}\frac{sT_w}{1+sT_w}\frac{1+sT_2}{1+sT_1}\frac{1+sT_4}{1+sT_3} = D_{pss}s \qquad (28)$$

with $s = j\omega_{area}$, where $F_{pssx}(s)$ is $F_{pssm}(s)$ or $F_{pssf}(s)$. Designing the stabilizer from Eq. (28) means that the stabilizer is set simply with a phase component to compensate the phase of $\dfrac{F_{pssx}(j\omega_{area})}{j\omega_{area}}$ such that $\Delta P_A(\Delta \boldsymbol{u}_{\boldsymbol{pss}}) = D_{pss}\Delta\dot{P}_A$ $(D_{pss} > 0)$. This ensures that the stabilizer provides a positive damping component to ΔP_A to suppress the line power oscillation.

III. Case Study

3.1 Case 1 - Design of a stabilizer on a STATCOM

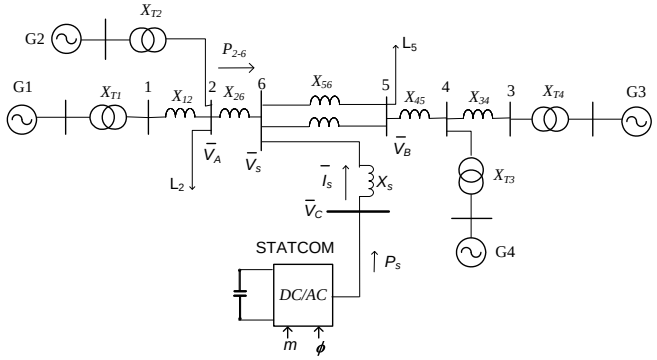

Figure 7 An example power system integrated with a PV power station

Figure 7 shows the configuration of a four-machine two-area power system, where a STATCOM is connected at node 6 along the tie line connecting two areas. This is the example power system (without the STATCOM) used in [18] for the study of power system inter-area power oscillations. It was also used as an example power system to demonstrate the suppression of inter-area power oscillations by FACTS stabilizers in [19,20]. Parameters of the power system are given in [21] and Appendix 2.

The STATCOM is installed to support the voltage at node 6. Although it does not have the capability to exchange the active power with the power system, a stabilizer can be added to the control loop of the modulation ratio signal *m* to improve the damping of power oscillation along the tie line [11,12,16]. At a steady-state operating condition when $P_{2\text{-}6} = 600MW$, the transfer function of the forward path of the stabilizer at the inter-area angular oscillation frequency is calculated to be

$$F_{pssm}(\mathrm{j}\omega_{area}) = -2.7242 - j1.3226 = 3.028\angle -154.1°$$

where $\omega_{area} = 3.4516$. Parameters of the stabilizer are set according to Eq. (28) and given in Appendix 2.

To validate the effectiveness of the stabilizer, Table 1 gives the computational results of the inter-area oscillation mode of the power system (other local oscillation modes are not listed) with and without the STATCOM stabilizer. Figure 8 shows the results of non-linear simulation of the power system when it was subject to a large disturbance: a three-phase-to-earth short circuit, at node 3 at the 0.2 second point of the simulation for a duration 100ms. From Table 1 and Figure 8 it can be seen that the stabilizer is designed successfully by using the phase compensation method. The inter-area power

oscillation is effectively suppressed by the stabilizer attached to the STATCOM.

Table 1 Inter-area oscillation mode of example powers system in case 1

Without the STATCOM stabilizer	-0.1166 ± j3.4516
With the STATCOM stabilizer	-0.4388 ± j3.1827

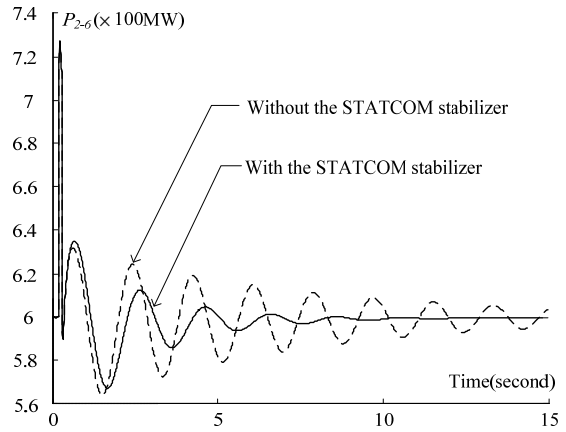

Figure 8 Results of non-linear simulation without and with the STATCOM stabilizer

3.2 Case 2 - Design of a BESS stabilizer

Figure 9 shows an example 16-machine power system where a BESS station is installed at node 69. Parameters of the system are given in [22] and Appendix 3. The mathematical model of the BESS proposed in [23] was adopted in this example. The BESS can exchange not only the reactive power, as the STATCOM does, but also the active power with the rest of the power system. Hence a stabilizer can be attached to the modulation ratio signal m in its AC voltage control loop. The stabilizer can also be attached to the modulation phase signal ϕ in the DC voltage control loop as shown in Figure 4. At a steady-state operating condition when $P_{27\text{-}69} = 100\text{MW}$, the two different stabilizers are designed separately by using the phase compensation method introduced in the previous section. Parameters of the BESS and attached stabilizers are given in Appendix 3.

Evaluation of the effectiveness of the stabilizers to suppress the inter-area power oscillation along the transmission line connecting node 27 and 69 is carried out by eigenvalue computation and non-linear simulation. Table 2 gives the inter-area oscillation mode with and without the stabilizers (other oscillation modes are not listed). The results from non-linear simulation (subject to a three-phase short circuit for 100ms duration at node 2 at the 0.2 second point of the simulation) are shown by Figure 10. Obviously the inter-area oscillation is effectively suppressed by either of the stabilizers which are designed locally using the phase compensation method.

The BESS rating is ±20MW. Figure 11 shows the simulation results of exchange of active power between the BESS and the rest of the power system. From Figure 11 it can be seen that when the stabilizer is implemented by controlling the modulation phase signal ϕ, the inter-area power oscillation is damped by controlling the exchange of active power between the BESS and the rest of the power system within the limit of the BESS rating.

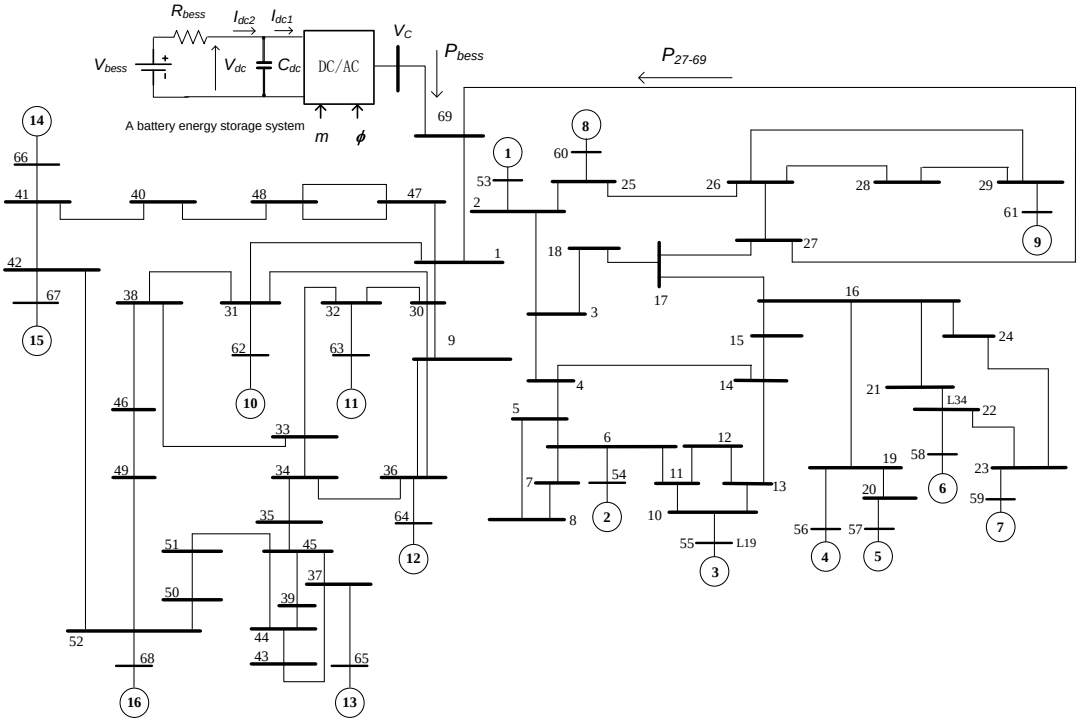

Figure 9 An example power system installed with a BESS unit

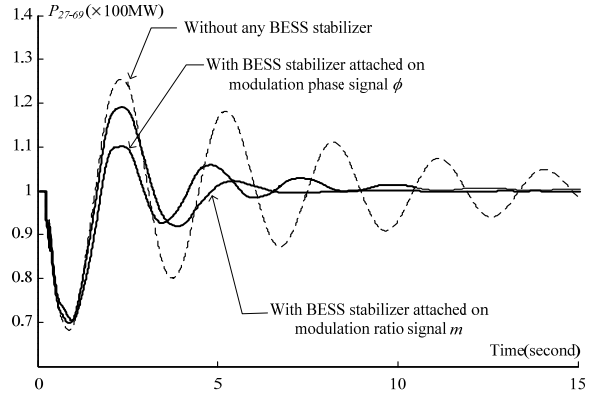

Figure 10 Results of non-linear simulation without and with the BESS stabilizers

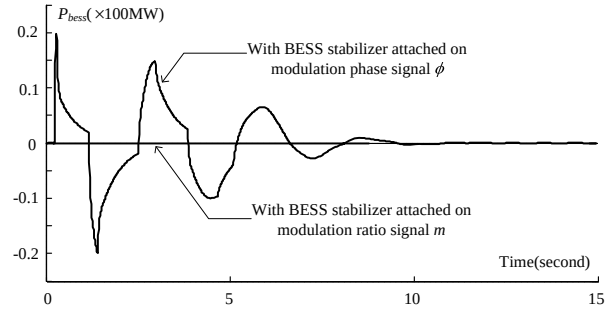

Figure 11 Results of non-linear simulation (exchange of active power between the BESS and the rest of the power system)

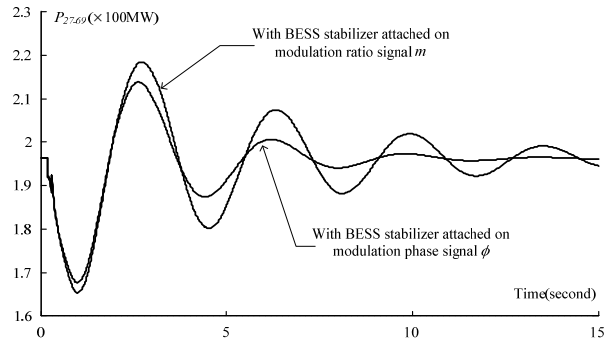

Figure 12 Results of non-linear simulation when the system operates at a higher loading condition of the transmission line

Table 2 Inter-area oscillation mode of example powers system in case 2

Without any stabilizer	$-0.1187 \pm j2.133$
With the BESS stabilizer added on m	$-0.4266 \pm j2.088$
With the BESS stabilizer added on ϕ	$-0.6919 \pm j2.307$

Table 3 Inter-area oscillation mode of example powers system in case 2 at a higher loading condition of the transmission line

With the BESS stabilizer added on m	$-0.1767 \pm j1.797$
With the BESS stabilizer added on ϕ	$-0.3649 \pm j1.843$

The robustness of the stabilizers to the variations in system loading conditions is examined by checking the control performance of the stabilizers at a higher loading condition of the transmission line $P_{27\text{-}69} = 196$MW. Table 3 and Figure 12 give the results of modal computation and non-linear simulation respectively. From Table 3 and Figure 12 it can be seen that the stabilizer attached to the modulation phase signal ϕ is more robust to the variations in system loading conditions.

When the stabilizer is added on the modulation phase signal ϕ, it operates in accordance with the BESS directly to absorb or inject the active power to damp the inter-area power oscillation, when it detects the excess or lack of the active power delivered along the transmission line. Hence the capability to damp the inter-area power oscillation is not excessively affected by the change in system loading conditions. When the stabilizer is added to the modulation ratio signal *m*, it operates by regulating the exchange of reactive power between the BESS and the rest of the power system to influence indirectly the variation of active power delivered along the transmission line. The extent of this indirect influence is related to the level of system loading conditions. Hence the effectiveness of the stabilizer is affected more by the variations of system loading conditions.

IV. Conclusions

This paper has proposed direct assessment of the damping component of inter-area power oscillations in a multi-machine power system as contributed by a stabilizer attached to a DC/AC converter based unit. The assessment has led to the application of the phase compensation method for the design of the stabilizer, which requires only a local linearized model of the DC/AC converter-based unit. Not only the proposed application in the paper is as simple as the design of a PSS by the phase compensation method in a single-machine infinite-bus power system, but also the design is localized without the need to obtain and validate the information and parameters of the entire multi-machine power system. Study case of two example power systems with a STATCOM and BESS installed is presented. The efficacy of the design of stabilizers attached to the STATCOM and BESS is confirmed by the results of modal computation and non-linear simulation.

V. References

[1] F. P. deMello and C. Concordia, "Concepts of synchronous machine stability as affected by excitation control", *IEEE Trans. on Power App. Syst.*, Vol. PAS-88, No.3, 1969, pp316-329

[2] W. G. Heffron and R. A. Phillips, "Effect of modern amplidyne voltage regulators on underexcited operation of large turbine generators, " *AIEE Trans. (Power Apparatus and Systems)*, Vol. 71, 1952, pp 692-697

[3] E. V. Larsen and D. A. Swann, "Applying power system stabilizers Part I-III", *IEEE Trans. Power App. Syst.*, Vol. 100, No. 6, 1981, pp3017-3046

[4] M. J. Gibbard, "Co-ordinated design of multimachine power system stabilisers based on damping torque concepts", *IEE Proc. Part C*, Vol. 135, No.4, 1988, pp276-284

[5] M. J. Gibbard, D. J. Vowles, and P. Pourbeik, "Interactions between, and effectiveness of, power system stabilizers and FACTS device stabilizers in multimachine systems", *IEEE Trans. on Power Systems*, Vol. 15, No.2, 2000, pp748-755

[6] M. J. Gibbard and D. J. Vowles, "Reconciliation of methods of compensation for PSSs in multimachine systems", *IEEE Trans. on Power Systems*, Vol. 19, No. 1, 2004, pp463-472

[7] H. F. Wang, F. J. Swift and M. Li, "A unified model for the analysis of FACTS devices in damping power system oscillations part II: multi-machine power systems", *IEEE Trans. on Power Delivery*, No.4, 1998, pp1355-1362

[8] H. F. Wang and F. J. Swift, "Multiple stabilizer setting in multi-machine power systems by the phase compensation method", *Int. J. of Electrical Power and Energy Systems*, No. 4, 1998, pp241-246

[9] G. Gurrala and I. Sen, "Power system stabilizers design for interconnected power systems", *IEEE Trans. on Power Systems*, Vol. 25, No. 2, 2010, pp1042-1051
[10] H. F. Wang, "Phillips-Heffron model of power systems installed with STATCOM and applications", *IEE Proc. Part C*. No.5, 1999, pp521-527
[11] N. Mithulananthan, C.A. Canizares, J. Reeve and G. J. Rogers, "Comparison of PSS, SVC, and STATCOM controllers for damping power system oscillations", *IEEE Trans. on Power Systems*, Vol. 18, No.2, 2003, pp786-792
[12] B. Bhargava and G. Dishaw, "Application of an energy source power system stabilizer on the 10 MW battery energy storage system at Chino substation", *IEEE Trans. on Power Systems*, Vol.13, No.1, 1998, pp145-151
[13] W. Du, H. F. Wang, S. J. Chen, J. Y. Wen and R. Dunn, "Robustness of damping control implemented by energy storage systems", *International Journal of Electrical Power and Energy Systems*, Vol. 33, No. 1, 2011, pp35-42
[14] N. G. Hingorani and L. Gyugyi, *Understanding the FACTS*, IEEE Press 2000
[15] Y. H. Song and A. T. Johns, *Flexible AC Transmission Systems*, IEE Press 1999
[16] Y. N. Yu, *Electric Power System Dynamics*, Academic Press Inc., 1983
[17] "Modeling of power electronics equipment (FACTS) in load flow and stability programs", *CIGRE T F 38-01-08*, 1998
[18] M. Klein, G. J. Roger and P. Kundur, "A fundamental study of inter-area oscillations in power systems", *IEEE Trans. on Power Systems*, Vol.6, No. 3, 1991, pp914-921
[19] X. Yang, and A. Feliachi, "Stabilization of inter-area oscillation modes through excitation systems", *IEEE Trans. on Power Systems*, Vol.9, No.1, 1994, pp494-502
[20] D. Z. Fang, Yang Xiaodong, Song Wennan and H. F. Wang, "Oscillation transient energy function and its application to design a TCSC fuzzy logic damping controller to suppress power system inter-area mode oscillations", IEE Proc. Part C, No.2, 2003
[21] P. Kunder, *Power System Stability and Control*, McGraw-Hill, 1994
[22] G. Rogers, *Power System Oscillations*. Kluwer Academic Publishers, 2000.
[23] Chen Shen, Zhiping Yang, M. L. Crow and S. Atcitty, "Control of STATCOM with energy storage device", *Proc. of IEEE Power Engineering Society Winter Meeting*, Vol. 4, Jan. 2000 pp2722 – 2728.

Appendix 1

From Figure 2 and Eq.(5) it can have

$$\bar{V}_A = jX(I_{Asx} + jI_{Asy}) + \bar{V}_a = -XI_{Asy} + V_a\cos\delta' + jXI_{Asx} + jV_a\sin\delta' \quad \text{(A1)}$$

where subscript x and y denotes the x and y component of the corresponding variable respectively in the common x-y coordinate of the power system. From Eq.(A1) it can be obtained that

$$I_{Asx} = -\frac{V_a\sin\delta'}{X}, I_{Asy} = \frac{V_a\cos\delta' - V_A}{X} \quad \text{(A2)}$$

Because

$$\bar{V}_A = jX_{As}\bar{I}_{As} + \bar{V}_s = jX_{As}(I_{Asx} + jI_{Asy}) - X_{As}I_{AsY} + V_{sx} + jV_{sy} \quad \text{(A3)}$$

it can be obtained from Eq.(A2) and (A3) that

$$V_{sx} = V_A + X_{As}I_{Asy} = V_A + X_{As}\frac{V_a\cos\delta' - V_A}{X} = \frac{X_{As}}{X}V_a\cos\delta'$$
$$+(\frac{X - X_{As}}{X})V_A = \frac{X_{As}}{X}(bV_B\cos\delta_{AB} + akmV_{dc}\cos\gamma) + (\frac{X - X_{As}}{X})V_A$$
$$V_{sy} = -X_{As}I_{Asx} = X_{As}\frac{V_a\sin\delta'}{X} = \frac{X_{As}}{X}(bV_B\sin\delta_{AB} + akmV_{dc}\sin\gamma) \quad \text{(A4)}$$

Linearization of Eq.(A4) is

$$\Delta V_{sx} = a_{1x}'\Delta V_{dc} + a_{2x}'\Delta m + a_{3x}'\Delta\gamma + a_{4x}'\Delta\delta_{AB} + a_{5x}'\Delta V_A + a_{6x}'\Delta V_B$$
$$\Delta V_{sy} = a_{1y}'\Delta V_{dc} + a_{2y}'\Delta m + a_{3y}'\Delta\gamma + a_{4y}'\Delta\delta_{AB} + a_{5y}'\Delta V_A + a_{6y}'\Delta V_B \quad \text{(A5)}$$

Because the modulation phase, ϕ, is the angle between $\bar{V}_s$ and $\bar{V}_c$, as given in Eq.(2), that is

$$\gamma = \phi + \varphi = \phi + \arctan^{-1}\frac{V_{sy}}{V_{sx}} \quad \text{(A6)}$$

from Eq.(A5) and (A6) it can have

$$\Delta\gamma = \Delta\phi + a_1'\Delta V_{dc} + a_2'\Delta m + a_3'\Delta\gamma + a_4'\Delta\delta_{AB} + a_5'\Delta V_A + a_6'\Delta V_B \quad \text{(A7)}$$

That gives

$$\Delta\gamma = a_g\Delta\phi + a_{g1}\Delta V_{dc} + a_{g2}\Delta m + a_{g4}\Delta\delta_{AB} + a_{g5}\Delta V_A + a_{g6}\Delta V_B \quad \text{(A8)}$$

By substituting Eq.(A8) into (A5) it can be obtained that

$$\Delta V_{sx} = a_{1x}\Delta V_{dc} + a_{2x}\Delta m + a_{3x}\Delta\phi + a_{4x}\Delta\delta_{AB} + a_{5x}\Delta V_A + a_{6x}\Delta V_B$$
$$\Delta V_{sy} = a_{1y}\Delta V_{dc} + a_{2y}\Delta m + a_{3y}\Delta\phi + a_{4y}\Delta\delta_{AB} + a_{5y}\Delta V_A + a_{6y}\Delta V_B \quad \text{(A9)}$$

By using Eq.(A9), linearizing Eq.(A6) it can have

$$\Delta\varphi = b_{1f}\Delta V_{dc} + b_{2f}\Delta m + b_{3f}\Delta\phi + b_{4f}\Delta\delta_{AB} + b_{5f}\Delta V_A + b_{6f}\Delta V_B \quad \text{(A10)}$$

In the x-y coordinate of the power system, $\bar{V}_s = V_{sx} + jV_{sy}$. Hence linearization of V_s can be obtained from Eq.(A9) to be

$$\Delta V_s = \frac{V_{sx0}}{V_{s0}}\Delta V_{sx} + \frac{V_{sy0}}{V_{s0}}\Delta V_{sy} = a_{1f}\Delta V_{dc} + a_{2f}\Delta m$$
$$+a_{3f}\Delta\phi + a_{4f}\Delta\delta_{AB} + a_{5f}\Delta V_A + a_{6f}\Delta V_B \quad \text{(A11)}$$

Appendix 2

Network parameters are given in [21]. Loading conditions are:

$$P_{G1} = 8.67\,p.u., P_{G2} = 7.00\,p.u., P_{G3} = 8.67\,p.u., P_{G4} = 7.00\,p.u.$$
$$L_2 = P_{L2} + jQ_{L2} = 9.67 - j1(p.u.), L_5 = P_{L5} + jQ_{L5} = 20.0 - j2.5(p.u.)$$;

Parameters of the STATCOM and stabilizer are:

$$C_{dc} = 1.0, K_{pac} + \frac{K_{ac}}{s} = 0.2 + \frac{5}{s}, K_{pdc} + \frac{K_{dc}}{s} = 0.2 + \frac{0.5}{s}$$
$$K_{pss} = 0.3281, T_1 = \mathrm{T}_3 = 0.01\mathrm{s}., \mathrm{T}_2 = T_4 = 0.5\,\mathrm{s}., T_w = 8\,\mathrm{s}.$$

Appendix 3

Because $I_{dc2} = \frac{V_{bess} - V_{dc}}{R_{bess}}$, where the equivalent resistance R_{bess} represents the power loss inside the BESS [23], the linearized model of the BESS as shown by Eq.(17) is $\Delta I_{dc2} = d_p\Delta V_{dc}$, $d_p = -\frac{1}{R_{bess}}$.

Parameters of the BESS

$$C_{dc} = 1.0, R_{bess} = 0.1, K_{pac} + \frac{K_{ac}}{s} = 0.2 + \frac{5}{s}, K_{pac} + \frac{K_{ac}}{s} = 0.2 + \frac{0.5}{s}$$

Stabilizer attached on m: Forward path $F_{pssm}(j\omega_s) = 1.242\angle 168.5^0$

Parameters $K_{pss} = -0.0088, T_1 = 0.9166\mathrm{s}., T_2 = 0.1\mathrm{s}., T_3 = 0.9166\mathrm{s}., T_4 = 0.1\mathrm{s}.$

Stabilizer attached on ϕ: Forward path $F_{pssf}(j\omega_s) = 1.675\angle 41.2^0$

$$K_{pss} = 0.01744, T_1 = 0.7299\mathrm{s}., T_2 = 0.3\mathrm{s}., T_3 = 0.7299\mathrm{s}., T_4 = 0.3\mathrm{s}.$$

Acknowledgement

The authors would like to acknowledge the support of the EPSRC UK-China joint research consortium (EP/F061242/1), the Science Bridge award (EP/G042594/1), UK, Jiangsu Power Company, China, and the Fund of Best Post-Graduate Students of Southeast University, China. Prof. Haifeng Wang is a member of the international innovation team of superconducting technology for electrical engineering at the Institute of Electrical Engineering, Beijing, China, sponsored by the Chinese Academy of Sciences, China.
Dr. Tim Littler has helped the editing and proof reading of the modified manuscript. The authors would like to thank the anonymous reviewers of the paper. Their comments and suggestions have significantly helped the improvement of the presentation of the work.

BIOGRAPHIES

Dr. Wendy DU is with the Southeast University, Nanjing, China and working as a Research Fellow at the Queen's University of Belfast. Her main research interests are power system stability analysis and control, including energy storage systems, FACTS and renewable power generation. Her contact e-mail address is ddwenjuan@qub.ac.uk